The research of space net control strategy based on the combination of fixed tearing belt and tether brake

Chunhui Zhan[1, a], Qingquan Chen[1, b], Qingbin Zhang[1, c]

[1] College of Aerospace Science and Engineering, National University of Defense Technology, Changsha 410073,China.

[a] 475524127@qq.com, [b] chenqingquan@nudt.edu.cn, [c] qingbinzhang@sina.com

Abstract. In order to solve the rebound motion of space tether net during deployment, a new control strategy based on adding tear tape in the plane and applying tether force out of the plane is proposed. The tether segment of the space tether net is discretized, and the lumped mass model is established. According to the mechanical characteristics of the tether, the system dynamic equation is derived. Then the simulation analysis is made from the perspective of evaluating the effect of the control strategy. Through simulation and comparison, it is found that the control strategy has obvious effect on restraining the rebound movement of the tether net.

Keywords: Multibody System Dynamics, Deployable Mechanisms, Modeling, Simulation, Control optimization, Multi-objective, flexible dynamics.

1. Introduction

At present, various space powers have successively carried out research on the active removal technology of space debris with tether nets. ESA proposed the Roger (Robotic Geostationary Orbit Restorer) project to catch abandoned satellites in geostationary orbit with tether nets [1-3]. A high altitude and low gravity test were conducted in 2015 [4]. NASA developed a tether-net catching mechanism named GRASP (Grapple, Retrieve, and Secure Load) [5-6], which uses tethers to form a net structure under the support of inflatable bars to catch loads. The EDDE (Electro-dynamic Debris Eliminator) project [7] funded by DAPPA of the United States plans to launch 12 spacecraft into space, each carrying 200 electromagnetic nets, for cleaning up LEO space debris. Japan put forward Furoshiki's new space tether net system [8-9], which is used to construct the future lightweight giant structure.

The dynamics of flexible space tether net has complex nonlinear characteristics, and scholars at home and abroad have carried out experimental and theoretical research on it. Zhang Qingbin et al. [10] checked and improved the dynamic model of space tether net through the ground test of tether net, and analyzed the difference of tether net deployment process in ground environment and space environment. Liu Haitao et al. [11] deduced the dynamic model of space tether net according to the different stress characteristics in the ground and space environment, and analyzed the influence of orbit height, capture direction and launch parameters on the deployment effect. Yang Fang et al. [12] studied the launch and deployment dynamics of space tether net based on the semi-mass damping spring model, and verified the model by experiments. Gao Xinglong et al. [13] used LS-DYNA software to simulate the contact and collision process when the space flying net caught the target. Gao Qingyu et al. [14] studied the secondary launching mode of the tether net, improved the pulling and unfolding process of the tether net, and verified the feasibility of this mode by combining simulation and experiment; Yu Yang, Li Jingyang et al. [15-17] established the finite element model of the flying net's projectile deployment by using software THUsolver and ABAQUS, respectively, studied the mechanical characteristics of the flying net in static and dynamic environments, and compared the deployment effects of the two folding methods of the flying net. Abroad, Lee et al. [18] used lumped mass model to simulate the movement process of underwater tether net, and compared it with the experiment qualitatively and quantitatively, which proved the effectiveness of this model. Takagi et al. [19] used lumped mass model to simulate the dynamics of tether net, compared with the experimental results, and analyzed the error. Minhe Shan et al. [20]

used the absolute node coordinate method and the lumped mass method to simulate the tether net deployment process, and made a comparative analysis. Eleonora M. Botta et al. [21] used lumped mass model to simulate the movement of space tether net, and modeled and analyzed the collision between tether net and target. The above models are used to simulate the space tether net, one of which is the lumped mass method, which has been widely used because of its good calculation efficiency and accuracy.

Through ground test and simulation calculation, it is found that after the tether net is expanded to the largest area, the net opening will be narrowed again and the tether net will rebound as a whole. This phenomenon greatly limits the effective working time and distance of the tether net. At present, there are few related studies on weakening or eliminating the rebound phenomenon of tether netting in China. In this paper, aiming at the rebound effect of tether during the deployment of tether net, a tether net configuration control strategy based on tether force and special binding belt is proposed, and the corresponding tether concentrated mass model and fixed tearing belt mechanical model are established, and the dynamic equation is derived. The motion characteristics of tether net without and with control strategy are compared and analyzed through simulation.

2.   Dynamic model of mesh control

2.1 Physical process

In this paper, the rebound control strategy of mass block traction tether net during launching and unfolding is studied. Tether net deployment mode, as shown in Fig. 1 to Fig. 3, the flexible tether net is folded and sealed in the net hold, and the four corners of the tether net are connected by four pilot mass; When the launching mechanism receives the launching instruction, the pilot mass will gradually unfold the tether net at a certain speed by the pilot riser and fly forward. Through ground test and simulation calculation, it is found that after the tether net is expanded to the largest area, the net opening will gradually shrink again and the tether net will rebound as a whole. This phenomenon greatly limits the effective working time and distance of the tether net. In this paper, in order to solve the problem of rebound movement during the deployment of the tether net, a control strategy of tether net configuration is proposed, which is to set a special binding belt at the diagonal lines of the tether net based on the in-plane movement of the tether net and to apply a towing tether force based on the out-of-plane movement of the tether net.
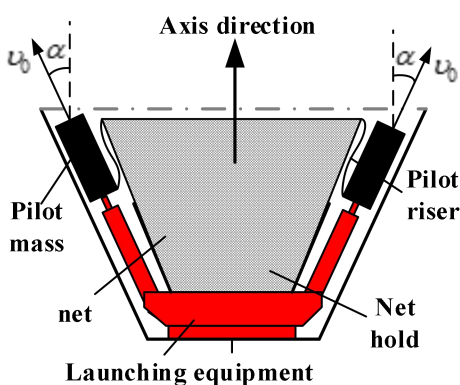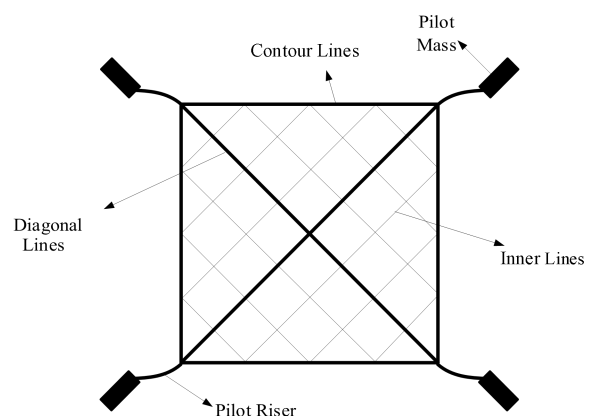

Fig. 1 Net casting mechanism   Fig. 2 Schematic diagram of tether net structure
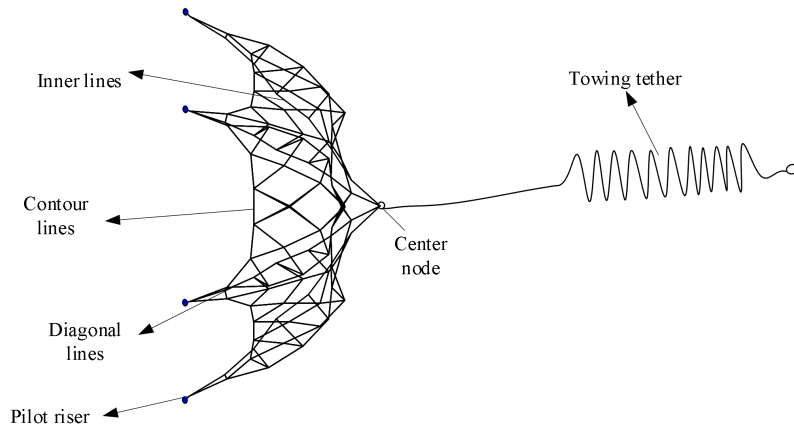
Fig. 3 Schematic diagram of tether net system structure

In the aspect of in-plane motion control, it is found by ground test and simulation calculation that the tether net will rebound when it is expanded to the largest area. The main reason is the elastic restoring force of the tether pulling the pilot mass, which leads to in-plane rebound. In order to consume the energy of the mass block in the surface of the tether net and learn from the simple control method of reducing the "straightening force" in the process of parachute straightening, this paper installs the "binding belt" on the diagonal lines of the tether net.

In the aspect of out-of-plane motion control, the "braking" control mechanism commonly used in the Tethered Satellite System (TSS) is used for reference to design the control mechanism for controlling the release of the connecting tether. In this mechanism, by adjusting the pressure acting on the connecting tether, the friction acting on the connecting tether can be changed, and the stable dynamic friction can be obtained through a very simple control mechanism.

2.2 Tether net dynamic model

According to the idea of discretization modeling, the tether net is discretized into several finite tether segments, and then the mass of each tether segment is concentrated at two ends, that is, nodes. Considering the special mechanical characteristics of the tether, it is assumed that the nodes are connected by a "spring", and the "spring" can only bear tension, but not pressure. At the same time, considering the damping effect of the tether, each unit is treated as a lumped mass damping spring, that is, a "Semi-Linear Springs and Dampers" model. Through the above discretization, as shown in Fig. 4, the whole space tether net is finally simplified as a multi-body system dynamic model connected by tether units. In the process of modeling, firstly, the elastic force and damping force of each element are calculated; Then calculate the external force on each unit, and then equivalent it to the associated node; Finally, the dynamic equations of each node are established, and the dynamic equations of the tether net system are obtained.
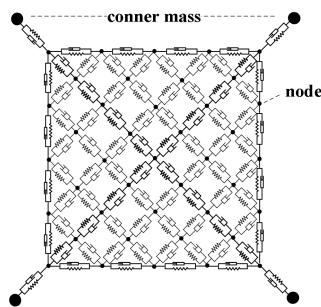

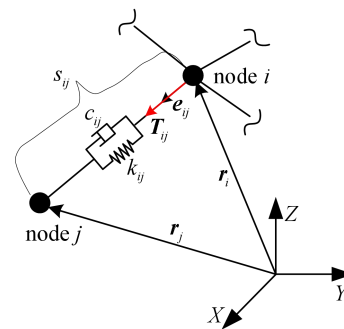
Fig. 4 Multibody system model of flexible net

Fig. 5 Semi-spring damper model of tether segment

Generally, the tension of tether segment can be approximately the sum of linear elasticity and linear damping, as shown in Fig. 5, the tension of s_{ij} is

$$T_{ij} = \begin{cases} k_{ij}(l_{ij} - l_{ij}^0) + c_{ij}\dot{l}_{ij} & l_{ij} > l_{ij}^0 \\ 0 & l_{ij} \leq l_{ij}^0 \end{cases} \tag{1}$$

Where, l_{ij} is the actual length of s_{ij} and $\dot{l}_{ij}$ is its change rate. The equivalent elastic coefficient and equivalent damping coefficient of s_{ij} are k_{ij} and c_{ij}, respectively.

As shown in Fig. 5, the nodes at both ends of s_{ij} are node i and node j, and the position vectors in the inertial system are r_i and r_j, respectively, so l_{ij} and $\dot{l}_{ij}$ can be calculated as follows.

$$l_{ij} = \left\| r_j - r_i \right\|, \quad \dot{l}_{ij} = \left(\dot{r}_j - \dot{r}_i \right) \cdot e_{ij} \tag{2}$$

Where e_{ij} is the unit vector from node i to node j, i.e.

$$e_{ij} = \frac{r_j - r_i}{\left\| r_j - r_i \right\|} \tag{3}$$

The equivalent elastic coefficient of s_{ij} is

$$k_{ij} = EA_{ij}/l_{ij}^0 \tag{4}$$

Where, E is Young's modulus, which is determined by material characteristics, and A_{ij} is the cross-sectional area of s_{ij}.

The equivalent damping coefficient of s_{ij} is

$$c_{ij} = 2\zeta\sqrt{m_{ij}k_{ij}} = 2\zeta\sqrt{\rho_{lij}EA_{ij}} \tag{5}$$

Where m_{ij} is the mass of the tether segment. ζ is the damping ratio, which depends on the material and weaving method of the tether, and the value is usually between 0 and 1.

As shown in Fig. 5, the mass of node i is m_i, and the position vector in the inertial coordinate system is r_i. According to Newton's Second Law, the dynamic equation of i can be expressed as

$$m_i\ddot{r}_i = \sum_{j \in R(i)} T_{ij} + \sum_{j \in R(i)} F_i^e \tag{6}$$

Where T_i and F_i^e are the tether tension and external force on the node i, respectively.

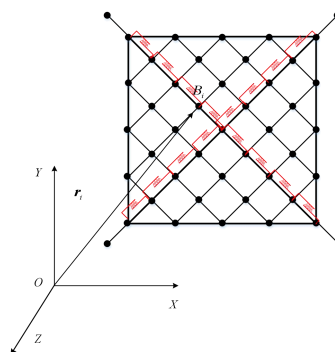## 2.3 Dynamic model of tear belt

Fig. 6 Illustration of space net multibody system model

In this paper, it is considered to set the tearing band control at the diagonal lines of the tether net. As shown in Fig. 6, under the assumption of concentrated mass, in order to study the dynamic model of controlling the tearing band, the mass of the diagonal lines node B_i of the tether net is m_i.

The F_i^a, internal force acting on node B_i, is the tension of the tether segment, and the F_i^e, external force, is the environmental force and the tearing force.

The external force on the tether node is provided by the space environment where the tether net is located and the constant tearing band, that is

$$F_i^e = G_i^e + S_i^e \qquad (7)$$

The space environmental forces are described in detail in reference [13]. The following mainly introduces the force of constant tearing band, S_i^e. The node on the diagonal lines of the tether net is subjected to a certain force, and the tearing force is

$$S_i^e = \sum_{j=1}^{h_i} e_{ji}^e S_{ji}^e \qquad (8)$$

Where, h_i is the number of constant tearing bands that act on B_i, S_{ji}^e is the value of the acting force of the constant tearing bands connecting B_i and B_j on the node B_i, and e_{ij} is the unit vector opposite to the elongation direction of the constant tearing bands, and its value is

$$e_{ji}^e = \begin{cases} \dfrac{v_j - v_i}{|v_i - v_j|} & \dot{l}_{ij} > 0 \\[2mm] 0 & \dot{l}_{ij} \leq 0 \end{cases} \qquad (9)$$

The force acting on both ends of the fixed tear tape is related to the density of stitches and the strength of stitches, and the specific value can be measured by the tensile test as shown in Fig. 7. According to the test and engineering experience, the stress and deformation of the constant tear zone can be approximated as the curve shown in Fig. 8.
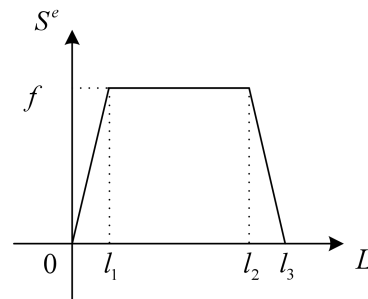

Fig. 7 Tension test of fixed-force tear belt   Fig. 8 Simplified force of fixed-force tear belt

In the Fig. 8, when the elongation of the fixed tear tape L is less than l_1, the F of the fixed tear tape monotonically changes with L and is reversible; When the elongation L is greater than l_1 and less than l_2, the tearing force is constant f and irreversible. When L is greater than l_3, the constant tear band breaks off. According to the test and engineering experience, this paper makes $l_1 = l_3/10$. According to the above characteristics of the tear tape, the tear force value S_{ji}^e is obtained as follows,

$$S_{ji}^e = \begin{cases} \dfrac{f}{l_1} l_{ij} & l_{ij} < l_1 \\[2mm] f & \dot{l}_{ij} > 0, l_1 \leq l_{ij} \leq l_2 \\[2mm] \dfrac{f}{l_3 - l_2}(l_{ij} - l_2) & \dot{l}_{ij} > 0, l_2 \leq l_{ij} \leq l_3 \\[2mm] 0 & \dot{l}_{ij} \leq 0 \\[2mm] 0 & l_{ij} > l_3 \end{cases} \qquad (10)$$

Due to the above-mentioned tearing band force loading form, some judgments are involved in numerical calculation, which is not conducive to programming and calculation, so least square fitting is adopted, and the fitting form is shown in the Fig. 9.
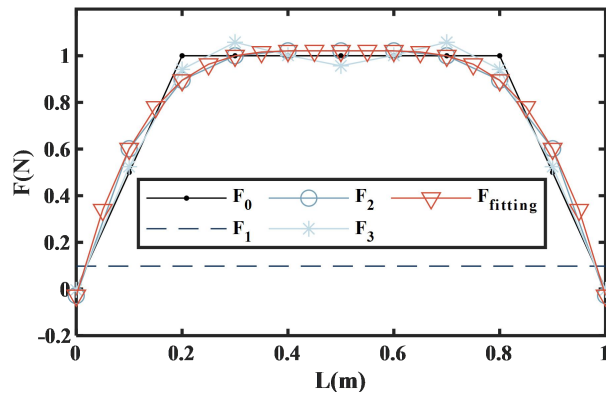

Fig. 9 Force fitting process of tearing band

2.4 Tethered force control

In this paper, a special lumped node N is added to the discrete flexible flying net structure, which is inside the release control mechanism at this stage of motion, while the neighboring node M_N is outside the release control mechanism. In the dynamic model, the capture platform also exists as a node and coincides with the node N. In the process of releasing the tether, only the node M_N is subjected to the friction force f acted by the control mechanism, and whether this friction force exists still needs to be judged as follows:
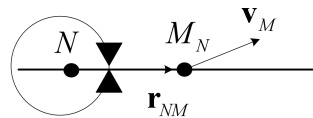

Fig. 10 Calculation of release control force of tether

When $\mathbf{r}_{NM} \cdot \mathbf{v}_M > 0$, that is, the movement direction of node M_N makes the distance between node M_N and node N increase, the control force exists. And the sensor is set to control the action range of the force for the tether net to expand to 20% to 60% of the designed area. The control force is

$$\mathbf{F} = -\frac{\mathbf{r}_{NM}}{\|\mathbf{r}_{NM}\|} f \tag{11}$$

Moreover, in the simulation calculation, when $\|\mathbf{r}_{NM}\| > l_{NM}$ during the movement, it is necessary to modify the special lumped node recorded above to be a node to the left of N. Tether force acts on the central node of the tether net.

3. Simulation analysis

3.1 Parameters setting

In this paper, if the diagonal lines length of the tether net is 10m, the design area of the tether net, that is, the area when it is fully unfolded, is 200m^2. According to the performance of the tether net to capture the target, the unfolded area of the tether net in the effective working area should not be less than 80% of the design area, that is, 160m^2. The other parameters are shown in Table 1. The four traction masses adopt the same launching speed and angle, which are 20m/s and 45° respectively.

Table 1. Simulation parameter

Parameters of tether net	Value
Number of nodes on edge line	10
Mass of single pilot mass	$1.0kg$
Density of edge lines, diagonal lines and pilot risers	$1288.9kg/m^3$
Diameter of edge lines, diagonal lines and pilot risers	$3e^{-3}m$
Elastic Modulus of edge lines, diagonal lines and pilot risers	$2e^{10}$
Density other tethers	$632.3kg/m^3$
Diameter of other tethers	$1e^{-3}m$
Elastic modulus of other tethers	$2e^{10}m$

In order to explore the influence of adding control strategies on the dynamic performance of tether net, this section sets control strategies as shown in Table 2 for simulation calculation.

Table 2. Simulation parameter

Parameters	Control added	No control added
Tethered force	$2N$	0
Force of fixed-force tear belt	$10N$	0

3.2 Simulation results and analysis

Under the same parameters in Table 1, the control parameters shown in Table 2 are set for the tether net. As it can be seen from Fig. 11, the deployment of the tether net has been greatly improved under the control strategy.
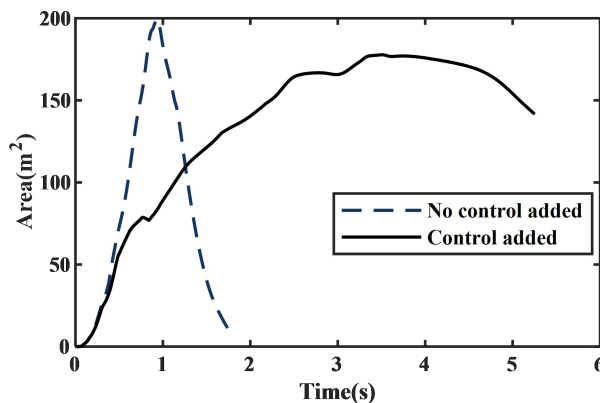

Fig. 11 Variation curve of the spread area of tether net with time

Fig. 11 describes the influence of the presence or absence of control strategy on the variation law of the unfolded area of the tether net with time. The tether net without control strategy bounces back quickly after expanding to the largest area, and the effective working time of the tether net is only 0.31s; The deployment speed of tether net with control strategy slowed down, and the effective working time was 2.46s, which was obviously improved. It should be noted that the curve jitter in the process of tether net deployment with control strategy reflects the influence of tether net system with mooring tether force control.
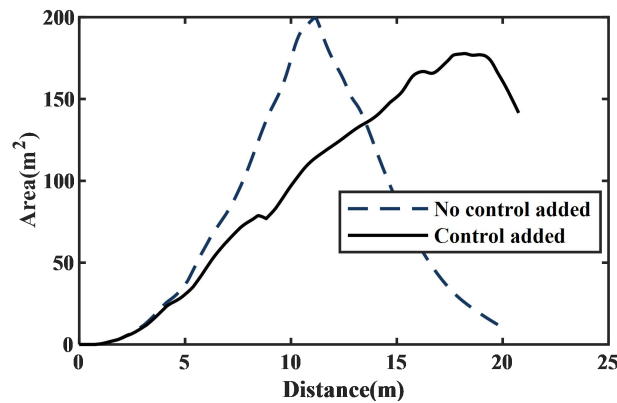
Fig. 12 Variation curve of the spread area of tether net with movement distance

Fig. 12 shows the influence of the presence or absence of control strategy on the variation of the spread area of the tether net with the flight distance of the tether net: the effective working distance of the tether net without control strategy is 2.8m; The effective working distance of the tether net with control strategy is 4.49m, which is slightly improved. The deployment process of the tether net is shown in Fig. 13, which describes the configuration state of the tether net in the same time interval. The upper part is the configuration without control and the lower part is the configuration with control, and the unit in the Fig. 13 is m. It can be seen that after adding control, the distance and time for the tether net to maintain an effective working state become longer.
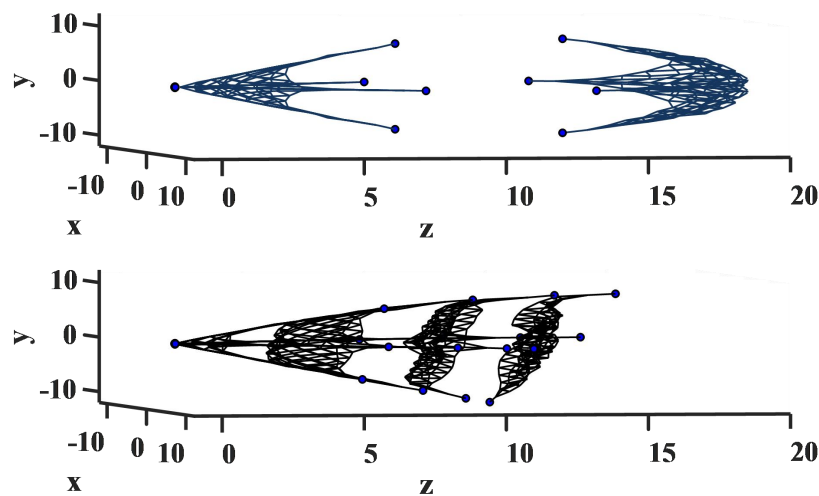

Fig. 13 Schematic diagram of tether net deployment process in the same time interval

From the above analysis, it can be seen that the tether net with this control strategy can be deployed well in space, and the effective working time of the tether net is increased by nearly 7 times. After the tether net is launched for 2.4s seconds, the tether net can fly stably in a space configuration suitable for capturing the target.

4. Summary

In this paper, in order to solve the problem of rebound movement in the process of tether net deployment, a control strategy of tether net type is proposed, which is to add a fixed binding band at the diagonal lines based on the in-plane movement of the tether net and apply a tether force based on the out-of-plane movement of the tether net. After the tether net is dispersed into finite segments, the corresponding tether concentrated mass model and the fixed tearing band mechanical model are established, and the dynamic equation of the tether net is deduced. Through simulation and comparative analysis, it is found that: (1) the control strategy can effectively weaken the rebound movement of the tether net and increase the effective working time and working distance during the

tether net deployment; (2) Adding the control of constant tearing band at the diagonal will reduce the maximum projected area of the tether net; (3) The application of mooring tether force control has a certain influence on the flying speed of the tether net during its deployment. The next work can further optimize the strength of the tearing belt, the installation position of the tearing belt and the setting of the mooring tether force.

References

[1] Bremen A S. Robotic Geostationary Orbit Restorer (ROGER) Phase a Final Report[R]. ESA, 2003.

[2] Kassebom M, Koebel D, Tobehn C, et al. ROGER—an Advanced Solution for a Geostationary Service Satellite[C]. The 54th International Astronautical Congress, Bremen, Germany, 2003.

[3] Bischof B, Kerstein L, Starke J, et al. ROGER—Robotic Geostationary Orbit Restorer[J]. Science and Technology Series, 2004, 109: 183-193.

[4] Michal D, Zuzanna D, Wojciech Golebiowski. Stereographic system for reconstruction of net flight trajectory[R]. ESA, 2015.

[5] Sorensen K. Conceptual Design and Analysis of an Mxer Tether Boost Station[J]. AIAA Paper, 2001, 3915: 1-11.

[6] Pearson J, Levin E, Oldson J, et al. EDDE, Electrodynamic Debris Eliminator: New Frontiers in Space Traffic Management[C]. The 4th IAASS Conference 'Making Safety Matter', Huntsville, USA, 2010.

[7] Carroll J A, Space Transport Development Using Orbital Debris[R]. Chula Vista, CA: Tether Applications, Inc., 2002.

[8] Nakasuka S, Aoki T, Ikeda I, et al. "Furoshiki Satellite"-a Large Membrane Structure as a Novel Space System[J]. Acta Astronautica, 2001, 48(5-12): 461-468.

[9] Kaya N, Iwashita M, Tanaka K, et al. Rocket Experiment on Microwave Power Transmission with Furoshiki Deployment[J]. Acta Astronautica, 2009, 65(1-2): 202-205.

[10] Zhang Qing-bin ,Sun Guo-peng, Feng Zhing-wei. Dynamics Modeling and Differentia Analysis Between Space and Ground for Flexible Cable net [J]. Journal of Astronautics, 2014, 35(8): 871-877.

[11] Gao Xing-long. Dynamic characteristics and simulation analysis of space net system. Hunan: National University of Defense Technology, 2011.

[12] Gao Qing-yu, Tang Qian-gang, Zhang Qing-bin. Dynamics Analysis of a Two-stage Projection Scheme of Space Nets System[J]. ACTA ARMAMENTARII, 2016,37(4): 719-726.

[13] Liu Hai-tao, Zhang Qing-bin, Yang Le-ping. The Deployment Dynamic Characteristics Analysis of Space Web System [J]. Journal of National University of Defense Technology, 2015, 37(3): 68-77.

[14] Yang Fang. Dynamics and Experimental Research on space net[D], Changsha: National University of Defense Technology, 2011

[15] Yu Yang, Baoyin He-xi, Li Jun-feng. Dynamic modeling and simulation of space net projectile[J]. Journal of Astronautics, 2010,31(5):1289-96.

[16] Li Jing-yang, Yu Yang, Baoyin He-xi.. Comparative study on two dynamics models of space net [J]. Journal of mechanics, 2011, 43(3): 542-50.

[17] Li Jing-yang, Yu Yang, Baoyin He-xi. Projectiong Parameters Optimization for Space Web systems[J]. Journal of Astronautics, 2012, 33(6): 823-829.

[18] Lee C W, Lee J H, Cha B J. Physical modeling forunderwater flexible systems dynamic simulation[J]. Ocean Eng, 2005, 32(3-4):331-347.

[19] Lee C W, Lee J H, Cha B J. Physical modeling forunderwater flexible systems dynamic simulation[J]. Ocean Eng, 2005, 32(3-4):331-347.

[20] Shan M H, Guo J, Eberhard G. Dynamics of Tethered-Net for Space Debris Capturing[J]. Acta Astronautica, 2017, 132:293-302.

[21] Eleonora M B, Inna S, Arun K M. Contact Dynamics Modeling and Simulation of Tether Nets for Space-Debris Capture. Journal of Guidance[J]. Control and Dynamics. 2017, 40(1):110-123.